Int. J. Electrochem. Sci., 15 **(2020)** 5179 – 5192, doi: 10.20964/2020.06.05

International Journal of ELECTROCHEMICAL SCIENCE
www.electrochemsci.org

Photocatalytic Self-Cleaning Electrochemical Sensor for 4-Nitrophenol detection

Jiabing Chen[1,2], Youluan Lu[1], Leshu Huang[1], Zhen Shi[2], Yin Zheng[1,2,] , Xinjian Song[2,*], Chenyi Wu[2], Zaikun Wu[3]*

[1] Hubei Key Laboratory of Biological Resources Protection and Utilization, Hubei, 445000, China
[2] Department of Chemistry, Hubei Minzu University, Enshi, Hubei 445000, China
[3] School of Chemical Engineering & Pharmacy, Wuhan Institute of Technology, Wuhan, Hubei 430073, China
[*]E-mail: zhengyin0617@163.com ; whxjsong@163.com

Received: 12 August 2019 / *Accepted:* 28 February 2020 / *Published:* 10 May 2020

Electrode fouling and passivation are the main reasons for attenuated the electrochemistry signals. In this work, a renewable electrode for determination of 4-nitrophenol (4-NP) which not only has excellent detection signals but also can be photo-catalytically refreshed to remain the selectivity and sensitivity was been created. The GO/TiO_2-CuTCPP composite material was characterized by Transmission electron microscopy (TEM), X-ray diffraction (XRD), electrochemical impedance spectroscopy (EIS), X-ray photoelectron spectroscopy (XPS), Fourier transform infrared spectra (FT-IR). The electrochemical behavior of 4-NP on GO/TiO_2-CuTCPP/GCE was investigated by cyclic voltammetry (CV) and square wave voltammetry (SWV) in 0.2 mol/L acetic acid buffer at pH 5.5. The result showed that the GO/TiO_2-CuTCPP/GCE exhibits the higher peak current and photo-catalytic activity to prone the self-cleaning ability. Under the optimal conditions, the oxidation current peak values linearly with the concentration of 4-NP ranging from 0.5 to 100 μmol/L, and the detection limit was 0.16 μmol/L (S/N = 3). Moreover, the sensors showed excellent renewable ability under visible light without damaging the electrode microstructure and attenuating electrochemical signals.

Keywords: graphene oxide, titanium dioxide, electrochemical sensor

1. INTRODUCTION

4-NP is a common chemical raw material which is widely used in agricultural and industrial processes and usually causes pollution[1]. It is significant to develop a simple and fast method for determination of 4-NP in environment water samples owing to its highly toxic, difficulties in degradation and persists in the environment[2]. Up to now, a lot of techniques was investigated to determine 4-NP,

for example spectrophotometry[3], fluorescence[4], gas chromatography[5], high performance liquid chromatography (HPLC)[6], capillary electrophoresis[7], electrochemical detection[8]. However, these methods often require expensive instruments, time-consuming operations, and complex sample preparation. Electrochemical method has attracted attention because of its low price, simple operation and time saving, high sensitivity and good selectivity. Therefore, electrochemistry becomes a reliable method for detecting 4-NP in the environment.

To improve sensitivity, chemically modified electrodes often require some common surface modification. Due to the unique nature of nanomaterials, it is often used to modify the electrode to increase the sensitivity of the electrode, such as MWNT[9], ionic liquid[10], gold nanoparticles[11], ZnO[12], quantum dot[13] and graphene[14]. Because of the large surface area, good electrical conductivity and high mechanical strength, the carbon materials are commonly used in the detection of phenolic substances in the electrochemistry sensors. However, the surface of electrode tend to be fouledand passivated by the intermediates products during the electrochemical reactions. The surface fouling and passivation of electrode tend to reduce the sensitivity and lifetime of the electrodes[15]. Some works have been reported about physical and chemical methods for cleaning electrode surfaces, such as physical polishing, acid washing, chemical and electrochemical methods to regenerate the electrode surface [16].

Inspired by photocatalysis in the environmental field, photodegradation is the easiest and lowest cost method for self-cleaning electrode surface fouling and passivation, some photocatalytic regeneration of electrodes have been reported [17,18]. However, most of photocatalytic self-cleaning electrochemical sensors photo-refreshing process occurred under the UV irradiation by the excellent photo catalysis of TiO_2[19]. Porphyrin is an effective sensitizer, which can expand the absorption range of TiO_2 light, enhance the separation efficiency of electron-hole pairs, and enhance the stability and photocatalytic activity of porphyrin-TiO_2. This allows the porphyrin-TiO_2 system to be used for photodegradation of 4-NP under visible light[20]. Meanwhile, the combination of graphene oxide and TiO_2 can promote electron transfer and enhance photocatalytic activity, which makes it feasible for the regeneration of electrode under visible light.

This paper reports an regeneration electrode based on ternary composite, which could self-cleaning in visible light. The composite materials GO/TiO_2-CuTCPP has been synthesized and dropped onto the electrode (GCE) to constituting 4-NP detection sensor. The electrochemical signal of 4-NP on this GO/TiO_2-CuTCPP/GCE was significantly higher than that of GCE, which was mainly due to the superior conductivity of the ternary material. As a result, the GO/TiO_2-CuTCPP/GCE showed wider detection range, higher sensitivity, and lower detection limit for detection 4-NP than some reported. The methoid could be applied to the determination of 4-NP in real sample with high recover. In addition, the electrode could be regenerated by the way of self-cleaning in visible light.

2. EXPERIMENT SECTION

2.1 Instruments

All the electrochemical signals including cyclic voltammetry (CV) and Square wave voltammetry (SWV) signals were emploied on a CHI660E Electrochemical Workstation with a three-

electrode system (Shanghai CH Instruments, China). Transmission Electron Microscopic (TEM) measurements were carried out with a JEM-2100 microscope. X-ray photoelectron spectroscopy (XPS) was recorded on ESCALAB 250 Xi instrument (ThermoFisher Scientific America). X-ray powder diffraction (XRD) was detected on a Shimadzu XRD-7000 (Shimadzu Japan) with Cu Kα radiation. Infrared spectral information was recorded on Avatar 370 FT-IR (Nicolet America) in the range of 400-4000cm^{-1}. KQ-2200 DE ultrasonicator (Kunshan Ultrasonic Instrument Co., Ltd, China)

2.2 Chemicals Reagents

All chemicals were analytical grade and used directly. Graphene oxide (GO) was obtained from JCNANO (China). Cu (II) meso-tetra (4-carbosyphenyl) porphine was purchased from Frontier Scientific, Inc. (the united states). TiO_2 was purchased from Degussa P25 (Evonik German). 4-Nitrophenol was purchased from LinEn Technology Development Co., Ltd (Shanghai China). Acetic acid buffer solutions were prepared from CH_3COONa and CH_3COOH, all solutions were configured using ultrapure water.

2.3 Preparation of GO/TiO-CuTCPP Composite material

The CuTCPP-TiO_2 composites were prepared in the following steps: Firstly, a certain amount (5 μmol/L) of CuTCPP was dispersed in 30 mL $CHCl_3$ solution, then 1 g Titanium dioxide (TiO_2) which had been heated to 120℃ and dried 2 h was transferred to the solution contained CuTCPP. After stirred for 4 h at room temperature, the solvent was removed under vacuum and dried to obtain the composites[21]. Then 10 mg of GO and 10 mg CuTCPP-TiO_2 composites were transferred into 10 mL of DMF for dispersed at the same time, and then sonicated for 3 h in KQ-2200 DE ultrasonicator to make the ternary composite material dispersed evenly. Thus, the GO/TiO_2-CuTCPP composites suspension was received.

2.4 Electrode treatment

GCE was with polished on the polishing cloth with 0.3 μm and 0.05 μm polishing powder until clean, and then the electrode surface was cleaned with nitric acid, ethanol, and ultrapure water for 3 minutes, respectively. 5 μL of GO/TiO_2-CuTCPP composites suspension was transferred and dropped onto the GCE surface, dried at 45℃ in the oven to remove solvent and formed a sensor.

2.5 Analytical Procedure

0.2 mol/L acetate buffer (pH = 5.5) was selected as electrolyte for 4-NP detection. After 70 s accumulation at 0 V, the square wave voltammetries were measured for 4-NP. CV and DPV scan range was -1.0V - 0.8V.

3. RESULTS AND DISCUSSION

3.1 Characterizations

The Surface topography and internal structure of GO and TiO_2-CuTCPP were investigated by TEM. As shown in Fig. 1A, 10 mg graphene oxide was exfoliated by ultra-sonically for 3 h in 10 ml DMF, the layered Graphene oxide nanosheets were observed, the fringe of GO and characteristic crumpled morphology can be explicitly identified. Fig. 1B showed that the graphene sheets were covered heavily with TiO_2 layer, which means that physical adsorption of TiO_2-CuTCPP on graphene oxide sheet was achieved with proper mechanical stirring and ultrasonic [22]. The evenly distribution of TiO_2-CuTCPP particles on the GO can improve the absorbance of visible light and the graphene single-layer structure will conducive to the transportation of electronics for photo-catalysis.

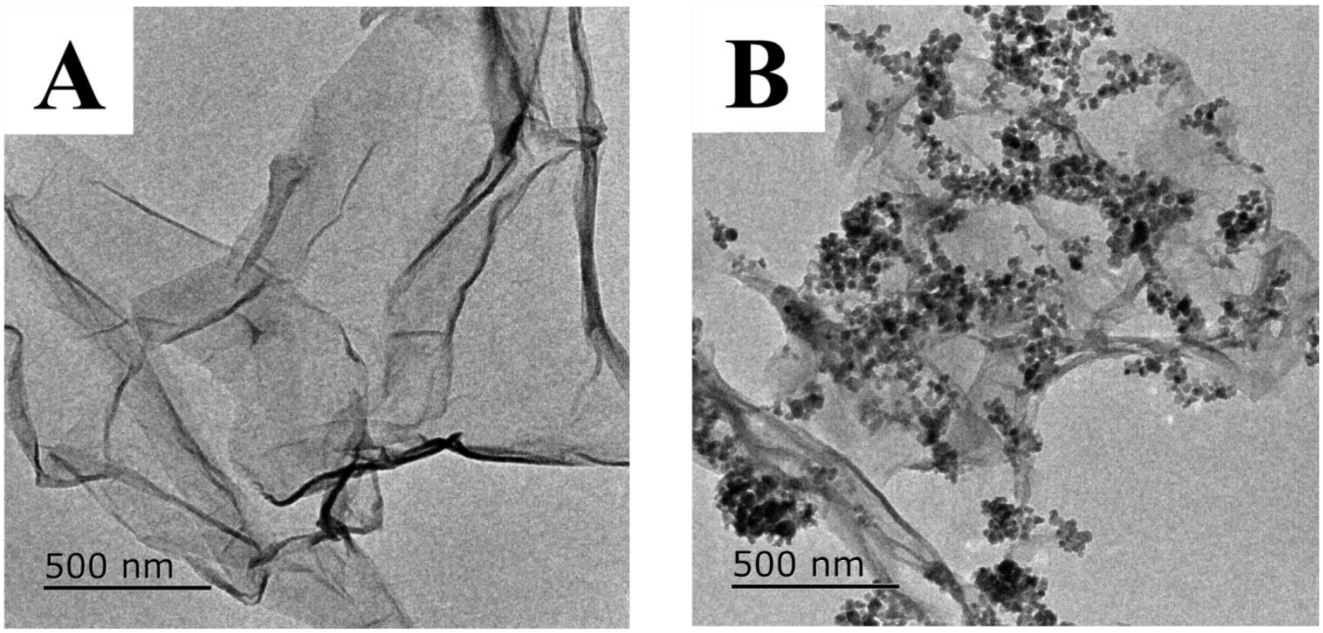

Figure 1. TEM images of Graphene-Oxide (A) and the GO/TiO_2-CuTCPP nanocomposite (B).

XPS was applied to investigate the chemical composition of GO/TiO_2-CuTCPP composites. As for O1s spectra in Fig. 2A, two obviously peaks can be observed at 529.6 eV and 531.7 eV, they were attributed to Ti-O and C-O bonds, which were derived from the reaction between the hydroxide of GO and the carboxyl group of CuTCPP [25]. Fig. 2B showed two peaks of $Ti2p^{3/2}$ and $Ti2p^{1/2}$ at 458.3 eV and 463.8 eV which proved the existence of TiO_2. Fig. 2C showed the high resolution XPS spectra of the C1s, the peaks of 284.0 eV and 285.9 eV were belonged to C-C bonds and C-O bonds. The reason why copper not detected in the figure may be caused by a low copper content. Moreover, from Fig. 2D, a peak of N1s appeared at 399 eV, and N1s originated from CuTCPP. The results indicated that copper porphyrin-sensitized TiO_2 has been successfully combined with GO. A lot of new peaks were observed in the spectra of GO/TiO_2-CuTCPP material, for example at 285.0 eV, it was also indicated perfect combination of composite materials of GO/TiO_2-CuTCPP [25].

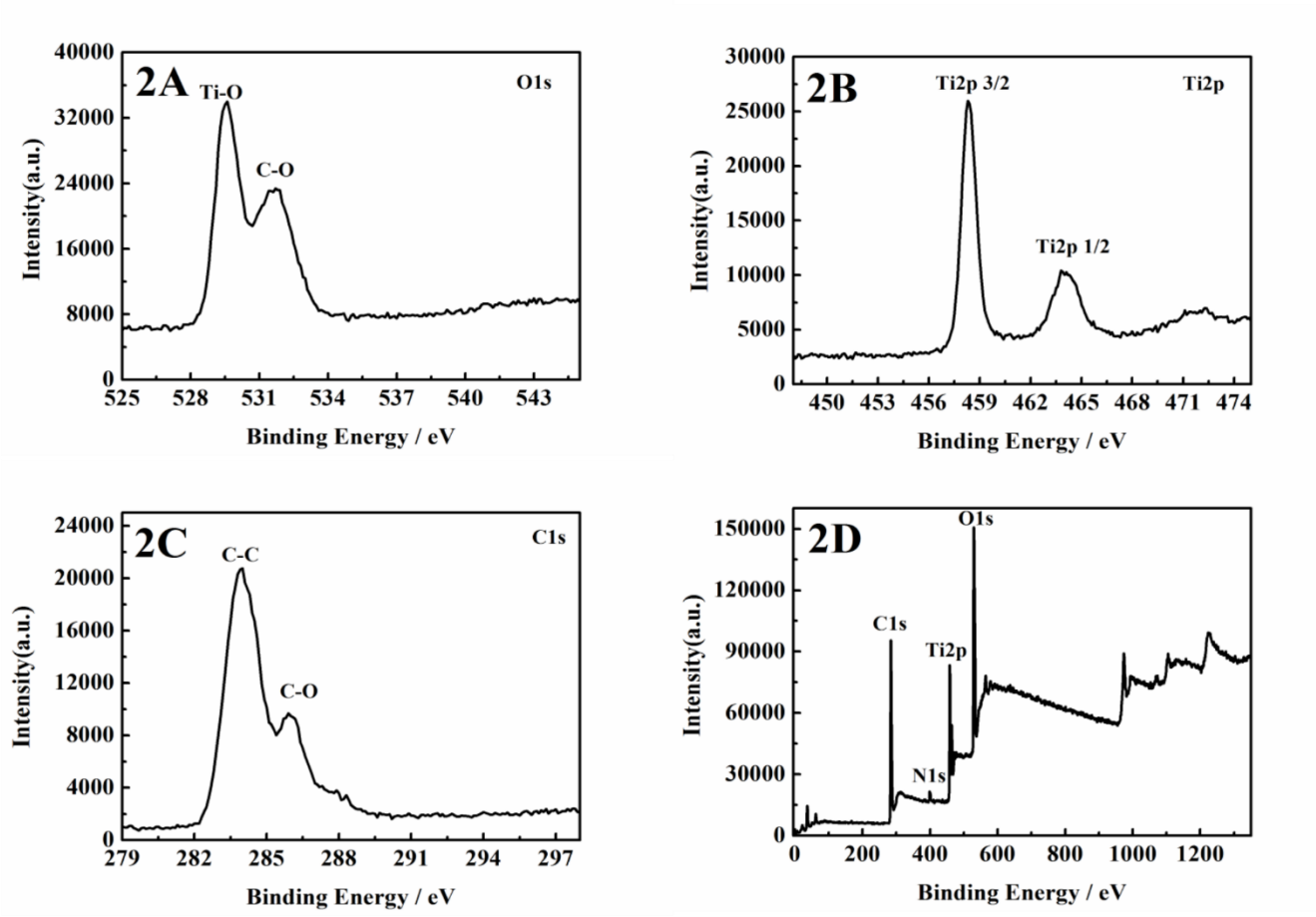

Figure 2. XPS (2D) and high-resolution XPS spectra of O1s (2A), Ti2p (C) and C1sfor the GO/TiO_2-CuTCPP nanocomposite.

The XRD patterns of TiO_2, TiO_2-CuTCPP and GO/TiO_2-CuTCPP nanocomposites were shown in Fig. 3. As shown in Fig. 3, there was almost no difference between TiO_2-CuTCPP and TiO_2. To be precise, the typical diffraction peaks (2θ= 25.3º, 37.9 º, 48.1º, 53.9º, 55.1º, 62.7º and 75.1º) of anatase titanium dioxide are showed in Fig.3 and which could be indexed to the (1 0 1), (0 0 4), (2 0 0), (1 0 5), (2 1 1), (2 0 4), (2 1 5) lattice planes reflection of anatase TiO_2 (JCPDS card 21-1272)[23,26]. The crystallinity of the TiO_2 was not changed after loaded by CuTCPP. After compounding with graphene oxide, an XRD peak appeared at 10.0º, corresponding to a (0 0 1) layer spacing of 0.78 nm, which owing to a lot of oxygen atoms inserted between the layers of graphene oxide [24].

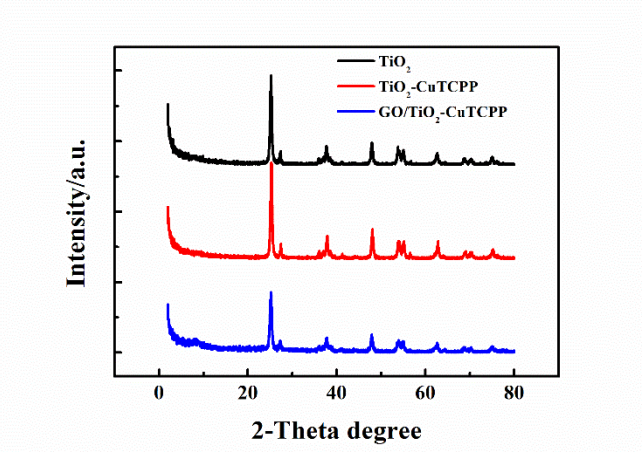

Figure 3. XRD patterns of TiO_2, TiO_2-CuTCPP and GO/TiO_2-CuTCPP nanocomposites.

The GO/TiO_2-CuTCPP was investigated by fourier transform infrared (FT-IR) technique in the Fig.4. The peaks at 3428 cm^{-1} and 1627 cm^{-1} can be attributed to the stretching vibrations and bending vibration of -OH on the surface of TiO_2 [25]. In addition, the bands around 521 and 650 cm^{-1} can be attributed to the characteristic absorption of Ti - O bonds in TiO_2. For both TiO_2-CuTCPP and GO/TiO_2-CuTCPP, bands were observed at 2903, 1500, and 1400 cm^{-1}, which can be attributed to the C-H, C = C characteristic vibrations of the carbon on the porphyrin ring on CuTCPP in the composite, and porphyrin Symmetrical stretching vibration on the carboxyl group. All these results proved that TiO_2 was sensitized by CuTCPP [27]. For GO and GO/TiO_2-CuTCPP, the absorption peaks at 3427 cm^{-1}, 1721 cm^{-1}, 1401 cm^{-1}, and 1052 cm^{-1} can be attributed to the OH tensile vibration on the GO, the C = O stretching, tertiary C - OH group stretching and CO stretching vibration. However, compared with GO, the peak corresponding to tensile vibration at C - OH 1401 cm^{-1} becomed narrower and weaker than GO/TiO_2-CuTCPP, which was mainly attributed to the weak interaction between -OH of GO and -OH on CuTCPP leads to the reduction of the hydroxyl groups on the surface of TiO_2. The results indicated that the ternary complexes have been combined with each other.

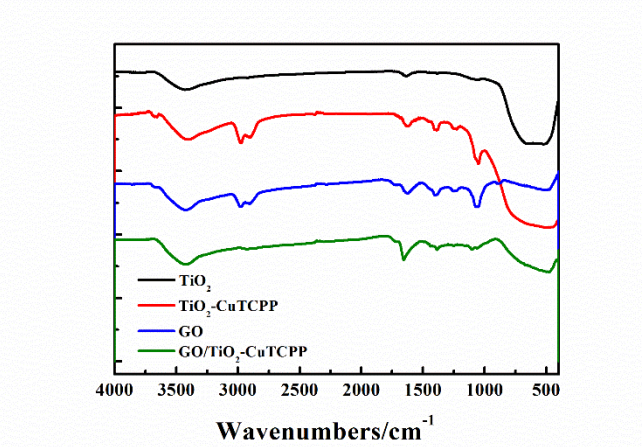

Figure 4. FT-IR patterns of TiO_2, TiO_2-CuTCPP, GO and GO/TiO_2-CuTCPP.

3.2. Electrochemical characterizations of GO/TiO_2-CuTCPP/GCE

The electrochemical characterizations of GO/TiO_2-CuTCPP/GCE was investigated by yclic voltammetry (CV) and electrochemical impedance spectroscopy (EIS). cyclic voltammetry (CV) was applied to inspect the electrochemical behavior of GO/TiO_2-CuTCPP/GCE towards in 0.1 mol/L KCl contained 5 mmol/L $[Fe(CN)_6]^{3-/4-}$. The cyclic voltammograms obtained for bare GCE (a), GO/GCE (b), GO/TiO_2-CuTCPP/GCE (c) were compared in Fig. 5A. The redox peak current value of the redox probe on GO/TiO_2-CuTCPP/GCE was much higher than that of GO/GCE and GCE. It was mainly owing to the higher electroactive surface area and good electronic conductivity of GO [30].

Fig. 5B showed the Nyquist plots for bare GCE (a), GO/GCE (b) and GO/TiO_2-CuTCPP/GCE (c). As shown in Fig 5B, GCE (c), GO/GCE (b) and GO/TiO_2-CuTCPP/GCE (a) all possessed a semi-circular arc in the high frequency region. The diameter of the semi-circular werc often represents the size of the resistance. The arc size of GO / TiO_2-CuTCPP / GCE (a) was significantly lower than GCE (c), and GO/GCE (b) was mainly due to the good electrical conductivity of GO and the electronic conductivity of Cu^{2+} in CuTCPP [31]. These results confirmed that the GO/TiO_2-CuTCPP/GCE have strong adsorptive capability for 4-NP owing to some of interaction between them such as hydrogen bonds and some hydrophobic force between GO and 4-NP, and 4-NP possessed the aromatic structure so that there are π-π stacking between them [32, 33]. Meanwhile, the specific surface area, the excellent electrical conductivity and the adsorption capacity of 4-NP were increasing because of TiO_2-CuTCPP attached to the surface of graphene, indicated that this electrode was promising for determination of 4-NP[34].

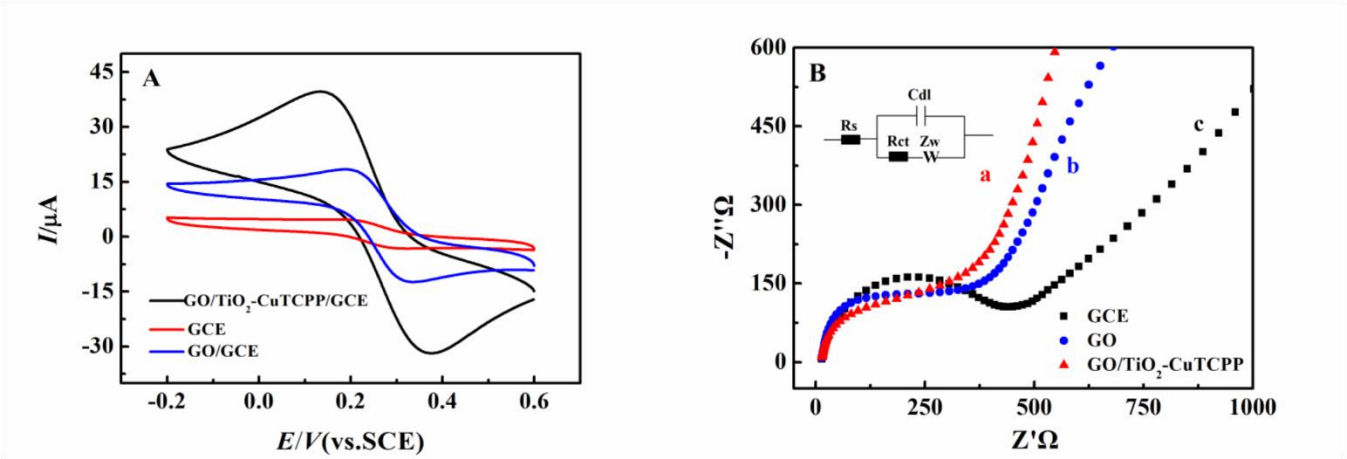

Figure 5. Cyclic voltammograms (A) and Nyquist plots (B) for different electrode.

3.3 Electrochemical Behaviors of 4-NP on electrode

Fig. 6 showed the electrochemical behavior of 4-NP on different electrodes with CV and SWV. As shown in Fig. 6A, the redox peaks of 4-NP in GO/TiO_2-CuTCPP/GCE was obviously higher than GCE and GO/GCE, this indicated that the composite is an effective mediator for the electrochemical oxidation of 4-NP [35]. The electrochemical signal of 4-NP on GO and GO-TiO_2 electrodes was mainly

attributed to the ability of GO to adsorb 4-NP [36]. Meanwhile, there were hydrogen bonds between GO and 4-NP and π-π stacking between them. These interaction forces enable GO and 4-NP to generate more electrochemical signals to improve the electrochemical detection effect [37,38]. As shown in Fig. 6A, the SWV curve of 4-NP on the composite electrode was also significantly higher than that of GO/GCE and GCE. Therefore, the oxidation peak of 4-NP can be selected to detect the 4-NP concentration.

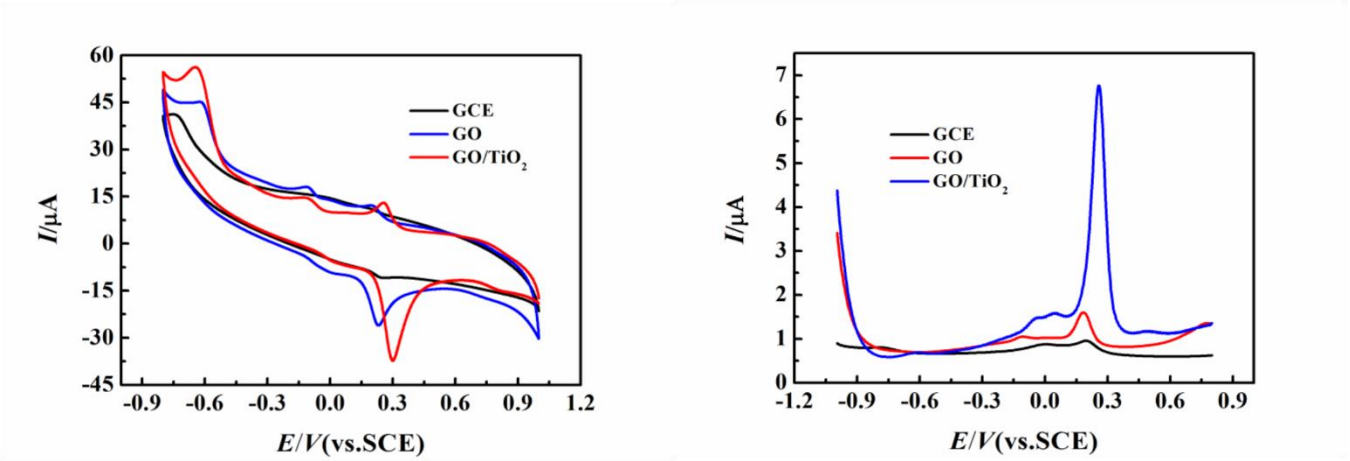

Figure 6. CV curves of 50 μmol/L 4-NP (A) and SWV curves of 10 μmol/L in pH 5.5 Acetic acid buffer solution on GCE, GO/GCE, GO/TiO_2-CuTCPP/GCE.

3.4. Optimization of experimental parameters for determination of 4-NP

3.4.1 Influence of pH

The experiment examined the influence of the electrode in different 0.2 mol/L buffer solutions (phosphate buffer solution, acetate buffer solution, borate buffer solution) on the detection of 4NP. The results showed that 4-NP had the best peak shape and highest peak values in the acetate buffer solution, so 0.2mol / L acetate buffer solution was selected as the supporting electrolyte. Fig. 7A showed the CV curves of 100 μmol/L of 4-NP in GO/TiO_2-CuTCPP/GCE versus buffer solutions of different pH values. As shown in the Fig. 7B, when the pH value increased from 3.5 to 5.5, the peak current value increased continuously with the increasd of pH. When the pH value increased from 5.5 to 6.5, the peak current value gradually decreased. Therefore, pH = 5.5 acetate buffer solution was chosen as optimal pH for the subsequent analytical experiments.

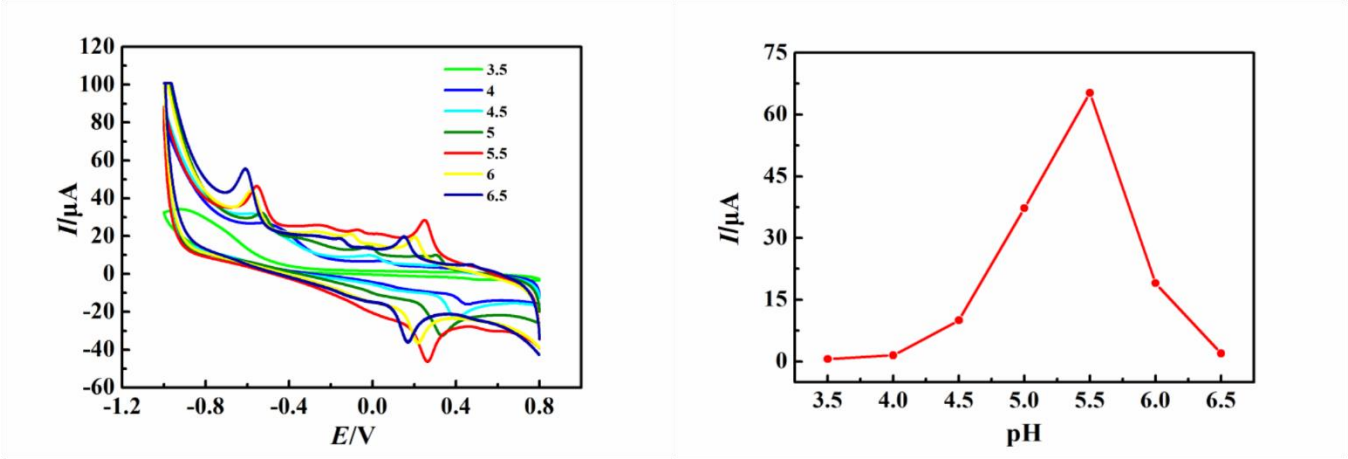

Figure 7. The effect of pH in the presences of 100 μmol/L 4-NP (A) and the effect of pH on peak current (B) .

3.4.2 Influence of scan rate

The electrochemical behaviors of 4-NP on GO/TiO_2-CuTCPP/GCE with different scan rates were investigated. As shown in Fig. 8A, the oxidation peak and reduction peak current values of 4-NP in GO/TiO_2-CuTCPP/GCE gradually increased with the increase of the scan rates range from 10 - 200 mV/s (a→g: 10, 40, 70, 100, 130, 160, 200 mV/s), as shown in Fig. 8B. a linear relationship between the peak current and the scan rates of 4-NP on GO/TiO_2-CuTCPP/GCE. the results show that the redox processes of 4-NP at GO/TiO_2-CuTCPP/GCE were controlled by adsorption [39,40].

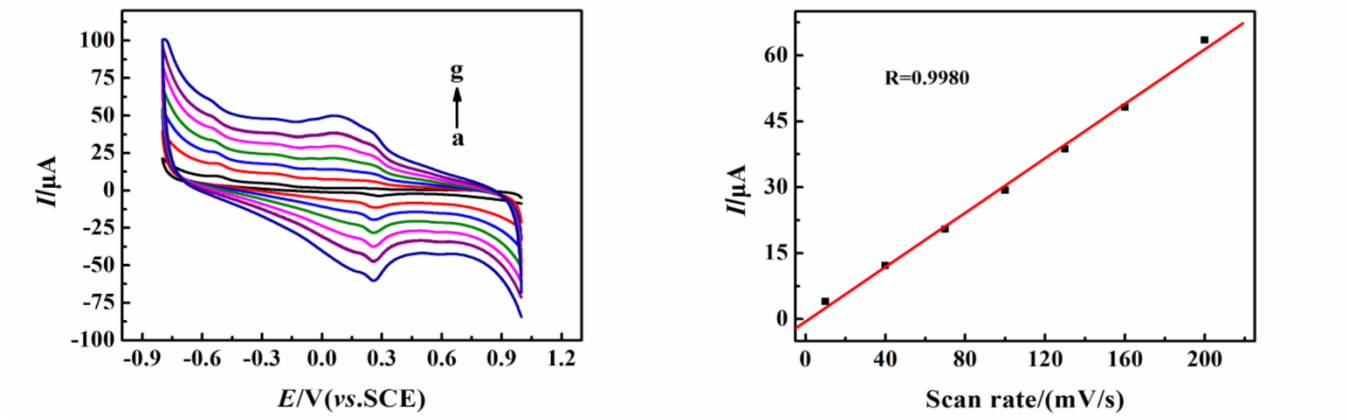

Figure 8. CV curves at different scan rates in the presence of 100 μmol/L 4-NP (A) and t Linear fit of oxidation peak current values and scan rates (B). Curves are obtained at 10, 40, 70, 100, 130, 160 and 200 mV/s, respectively.

3.4.3 Influence of accumulation potential and time

Influence of the accumulation potential and time on the square wave voltammetric (SWV) response for 4-NP on GO/TiO_2-CuTCPP/GCE were investigated. A solution of 0.02 mmol/L of 4-NP

was investigated in a phosphate buffer solution at pH 5.5, when the fixed accumulation time was 70 s, the effect of the peak current value of 4-NP on GO/TiO_2-CuTCPP/GCE under different accumulation potentials was investigated. The results were shown in Fig. 9A. when the accumulation time range from -0.6 – 0 V, the peak current values gradually increased, and when the accumulation potential was from range from 0 - 0.6, the peak current value gradually decreases, so the potential of 0V is selected as the best enrichment potential. As shown in Fig. 9B, when the fixed accumulation potential was 0 V, the accumulation time was increased to 70s, the peak current value gradually increased and reached to maximum value, so the optimal enrichment time was selected as 70s. Therefore, 0 V and 70 s were setted to the optimum parameters for the following experiments.

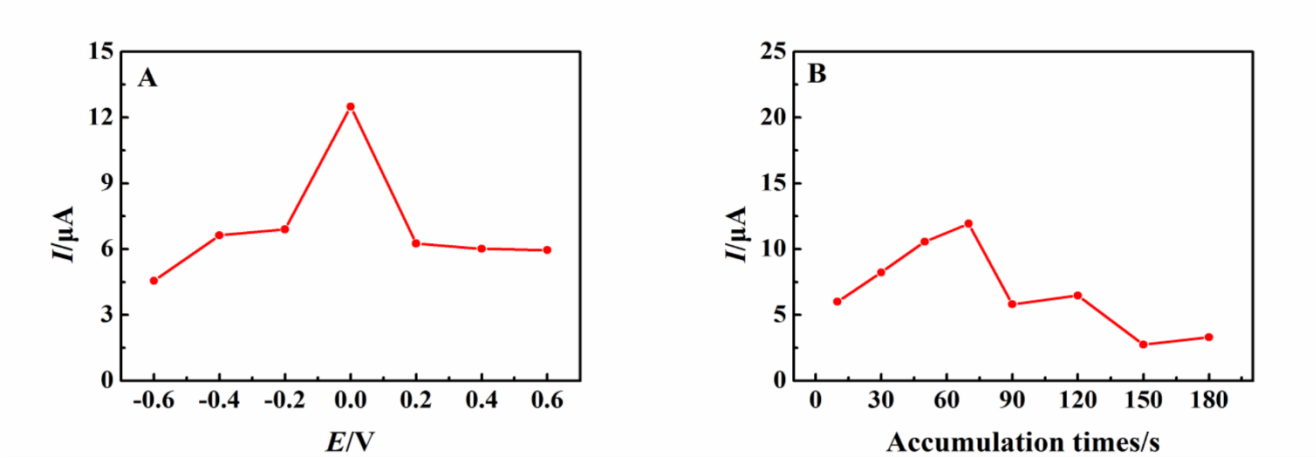

Figure 9. The effect of accumulation potential (A) and accumulation time (B) on the oxidation peak currents of 10 μmol/L 4-NP on SWV current response at GO/TiO_2-CuTCPP/GCE.

3.5 Sensitivity

Sensitivity was a significant part of the constructed electrochemical sensor. SWV was applied to investigate the relationship of oxidation currents values (I_p) and concentrations (c). As shown in Fig. 10A. For detection of 4-NP, the oxidation peak current increased linearly with its concentration (c) in the range from 0.5 to 100 μmol/L (a→k: 0, 0.5, 1, 2, 4, 8, 10, 20, 60, 80, 100 μmol/L), and the linear regression equation was: I_p =1.10992 c+12.45 (I_p in μA, c in μmol/L, R=0.9925) (Fig. 10B). The limit of detection (LOD) value was 0.16 μmol/L (S/N = 3), compared to the reported electrochemical sensors, GO/TiO_2-CuTCPP/GCE possessed wider detection range and lower detection limit (Table. 1). The main intent was to manufacture a visible light photocatalytic self-cleaning electrochemical sensor under visible light. Owing to TiO_2's conductivity was not as good as other nanomaterials, the LOD of this electrochemical sensor is higher than some developed sensors. With the U.S. Environmental Protection Agency regulates the maximum limit of 4-NP in drinking water to 0.43 μmol/L [2], it indicated that the sensitivity of GO/TiO_2-CuTCPP/GCE was high enough for sample analysis with reliable results.

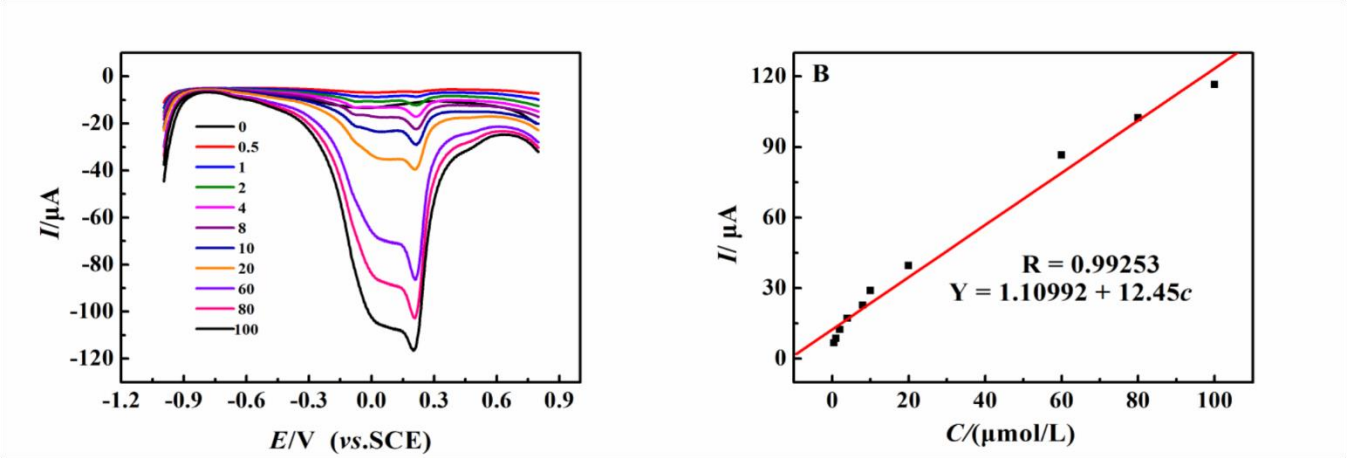

Figure 10. SWV curves of GO/TiO_2-CuTCPP/GCE in pH 5.5 a series of concentrations of 4-NP (a→k: 0, 0.5, 1, 2, 4, 8, 10, 20, 60, 80, 100 μmol/L) and the calibration curve for 4-NP determination.

3.6 self-cleaning capability of GO/TiO_2-CuTCPP/GCE

The photo-catalytic self-cleaning process of GO/TiO_2-CuTCPP/GCE based on GO-TiO_2 was described as follow and showed in Fig. 11: 10 μmol/L 4-NP were detected by GO/TiO_2-CuTCPP/GCE, the contaminants were left on the surface of the electrode after determination, test the contaminants currents, then a drop of ultrapure water was dropped onto the surface of GO/TiO_2-CuTCPP/GCE. Later, the GO/TiO_2-CuTCPP/GCE was transferred under visible light with the illmination for 60 min and 120 min. Some active intermediate would generate by the reaction between TiO_2 with H_2O and O_2 owing to porphyrin could be the efficient sensitizers to harvest light on the surface, the resulting substances such as •OH, O_2^- and H_2O_2 could oxygenolysis the organic pollutants and intermediates on the electrode surface. (e.g. 4-NP adsorbed on the electrode's surface) [41-44]. The CuTCPP–TiO_2 composite photo-catalyst displayed a high removal rate in 4-NP photo-catalytic degradation. After 120 min photocatalytic reaction, the oxidation peak current values in blank acetate buffer were nearly closed to 0 μA, which indicated that the 4-NP adsorped on the surface of electrode were completely photodegraded, and the peak current declines a little when 4-NP was added again.

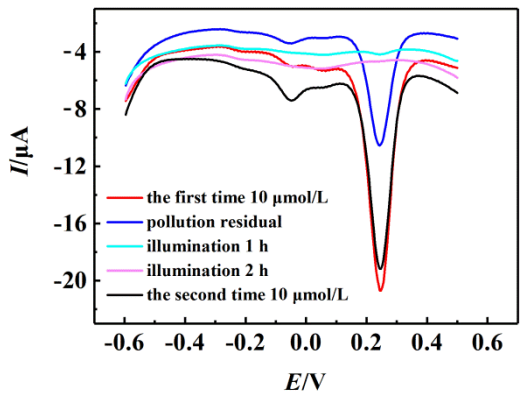

Figure 11. Photocatalytic self-cleaning reusability curves for GO/TiO_2-CuTCPP/GCE in the presence of 10 μmol/L 4-NP.

3.7 Interference effects

The experiment further investigated the effects of coexisting substances on GO/TiO_2-CuTCPP/GCE for 4-NP detection. In the presence of 10 μmol/L 4-NP, 500 μmol/L of Na^+ , Mg^{2+}, Al^{3+} , Ca^{2+}, Zn^{2+} , Ni^{2+} , Fe^{3+}, Cu^{2+}, Cl^- , CO_3^{2-} , SO_4^{2-} and NO_3^- did not interfered the results (peak current change <5%); 100 μmol/L of 2,4-dinitrophenol, pyrocatechol, hydroquinone, o-nitrobenzoicid, m-nitrobenzoic acid and p-nitrobenzoic acid also did not interfered the signal (peak current change <5%); However, 50 μmol/L of phenol, 2-nitrophenol and hydroxyphenol were interfered the results. Thus, these results indicated that GO/TiO_2-CuTCPP/GCE possessed a good selectivity for 4-NP.

Table. 1 Comparison of linear ranges and detection limits of 4-NP between different electrodes

Electrode material	Linear range (μmol/L)	Detection limit (μmol/L)	References
hydroxyapatite nanopowder	1.0 - 300	0.6	[45]
multiwalled carbon nano-tube (MWNT) /1-butyl-3-methylimidazolium tetrafluoroborate/chitosan	0.1-20	0.1	[46]
tmaePcCo/CNT	1.0-1000	0.2	[47]
MWCNT	1.0-30	0.12	[48]
GO/TiO_2-CuTCPP	0.5-100	0.16	This work

3.8 real sample detection

In order to investigate the application ability of the GO/TiO_2-CuTCPP/GCE in real sample, standard adding method was employed by adding 4-NP in tap water. The result was shown in table. 2, the recoveries of all samples were between 96.2% and 102.3% and the RSD values were between 2.3 and 4.2. It indicated that the modified electrode GO/TiO_2-CuTCPP/GCE can be used for the 4-NP detection in real water samples.

Table. 2 Determination results for 4-NP in tap water

Sample	Added (μM)	Found (μM)	Recovery (%)	RSD (%)
	4-NP	4-NP	4-NP	4-NP
1	1	0.962	96.2	2.3
2	10	10.23	102.3	3.1
3	50	48.63	97.3	4.2

4. CONCLUSIONS

A ternary composite material based on graphene oxide, TiO_2 and copper porphyrin with low cost and simple preparation method was prepared and a photo-regeneration electrochemical sensor for 4-

nitrophenol was prepared by one-step drop coating method. Under the optimal conditions, the sensor has good electrochemical response to 4-NP, and it can achieve photoregeneration of electrochemical sensor platform under illumination. This work provides a new idea for the design of regenerative electrochemical sensors.

ACKNOWLEDGMENTS
This work is supported by the National Natural Science Foundation of China (No. 21561011), the start-up Foundation for doctor of Hubei Minzu University (No. MY2013B027) and Hubei Key Laboratory of Biologic Resources Protection and Utilization (Hubei University for Nationalities)

References

1. Y. B. Zeng, Y. Zhou, T. S. Zhou, G.Y. Shi, *Electrochim Acta*., 130 (2014) 504.
2. A. Rana, A.N. Kawde And M. Ibrahim, *J Electroanal Chem*., 820 (2018) 24.
3. T. Muhammad, O. Yimit, Y. Turahun, K. Muhammad, Y. Uluda And Z. Zhao, *J Sep Sci*., 37 (2014) 1873.
4. G. Hashem, G. Ahmed,R. B. Laíño, J. A. G. Calzón And M. E. D. García, *Microchim Acta*., 182 (2015) 51.
5. F. Jaber, C. Schummer, J. A. Chami, P. Mirabel And M. Millet, *Anal Bioanal Chem*., 387 (2007) 2527.
6. Y. L. Zheng, D. Liu, H. Xu, Y. L. Zhong, Y. Z Yuan, L. Xiong And W. Li, *Int Biodeter Biodegr*., 63 (2009) 1125.
7. X. F. Guo, Z. H. Wang And S. P. Zhou, *Talanta*., 64 (2004) 135.
8. Y. H. Tang, R. Huang, C.B. Liu, S. L. Yang, Z. Z. Lu And S. L. Luo, *Anal Methods*,. 5 (2013) 5508.
9. A. Arvinte, M. Mahosenaho, M. Pinteala, A. M. Sesay And V. Virtanen, *Microchim Acta*., 174 (2011) 337.
10. S. Wei, M. X. Yang, Q. Jiang And J. Kui, *Chinese Chem Lett*., 19 (2008) 1156.
11. Y. Y. Tang And P. Y. Chen, *J Chin Chem Soc-Taip*., 58 (2011) 723.
12. B. Thirumalraj, C. Rajkumar, S. M. Chen And K. Y. Lin, *J Colloid Interface Sci*., 499 (2017) 83.
13. Y. G. Wu And F. Ran, *J Power Sources*., 244 (2017) 1.
14. Y. H. Zhang, L. H. Wu, W. Lei, X. F. Xia, M. Z. Xia And Q. L. Hao, *Electrochim Acta*., 146 (2014) 568.
15. A. Ghanam, A. A. Lahcen And A. Amine, *J Electroanal Chem*., 789 (2017) 58.
16. D. C. Thornton, K. T. Corby, V. A. Spendel, J. Jordan, A. Robbat, D. J. Rutstrom, M. Gross And G. Ritzler, *Anal Chem*., 57 (1985) 150.
17. Y. Wei, Q. Zeng, Q. Hu, M. Wang, J. Tao And L. Wang, *Biosens Bioelectron.*, 99 (2017) 136.
18. X. L. Zhu, Y. Y. Chen, C. Feng, W. Wang, B. Bo, R. Ren And G. Li, *Anal Chem*., 89 (2017) 4131.
19. V. Pifferi, G. Soliveri, G. Panzarasa, G. Cappelletti, D. Meroni And L. Falciola, *Anal Bioanal Chem*., 408 (2016) 1.
20. W. Y. Ma, J. Li, J. Z. Liu And F. Meng, *Chinese J Chem*., 31 (2013) 230.
21. M. M. Yu, J. Li, W. J. Sun, M. Jiang And F. X. Zhang, *J Mater Sci*.,49 (2014) 5519.
22. K. F. Zhou, Y. H. Zhu, X. L. Yang, X. Jiang And C. Z. Li, *New J Chem*., 35 (2010) 353.
23. S. J. Wang, H. L. Yu, S. Yuan, Y. Zhao, Z. Y. Wang, J. H. Fang, M. H. Zhang And L. Y. Shi, *Res Chem Intermediat*., 42 (2015) 3775.
24. X. Zhao, Y. Wang, W. H. Feng, H. T. Lei And J. Li, *Rsc Adv*., 7 (2017) 52738.
25. M. Wei, J. M. Wan, Z. W. Hu , Z. Q. Peng And B. Wang, *Appl. Surf. Sci*., 377 (2016) 149.
26. Q. Tao,B. W. WAng, X. L. Wang, X. L. Yan And L. G. Chen, *Appl. Surf. Sci.*, 490 (2019) 546.
27. C. H. Ruan , L. F. Zhang, Y. L. Qin, X. Chen, X. B. Zhang, J. M. Wan, Z. G. Peng, J. J. Shi, X. Y. Li

And L. N. Wang, *Mater. Lett.*, 141 (2015) 362.
28. W. Zhang , C. Wang , X. Liu And J. Li, *J. Mater. Res. Technol.*, 32 (2017) 2773
29. S. J. Parikh , J. D. Kubicki , C. M. Jonsson, C. L. Jonsson, R. M. Hazen, D. A. Sverjensky And D. L. Sparks, *Langmuir.*, 27 (2011) 1778.
30. E.Casero. A. M.Parra-Alfambra, M. D. Petit-Domínguez, F. Pariente, E. Lorenzo And C. Alonso, *Electrochem. Commu*., 20 (2012) 63-66.
31. M. Faraji, R. Hasanzadeh, *Energy Technol.*, 5 (2017) 1998.
32. Y. H. Tang , R. Huang , C. B. Liu, S. L. Yang, Z. Z. Lu And S. L, Luo, *Anal. methods*, 5 (2013) 5508.
33. B. Lang, H. K. Yu, *Chin Chem Lett.*, 2 (2017) 417.
34. A. Shokri , K. Mahanpoor And D. Soodbar, *J. Environ. Chem. Eng.*, 4 (2016) 5.
35. W. C. Peng, Y. Chen And X. Y. Li, *J. Hazard. Mater.*,309 (2016) 173.
36. Y. B. Zeng, Y. Zhou, T. S. Zhou And G. Y. Shi, *Electrochim. Acta*, 130 (2014) 504.
37. C. Sarkar, S. K. Dolui, *Rsc Adv.*, 5 (2015) 60763.
38. S. A. Zaidi, J. H. Shin, *Rsc Adv.*, 2015, 5 (2015) 88996.
39. G. Bharath, V. Veeramani, S. M. Chen, R. Madhu, M. M. Raja, A. Balamurugan, D. Mangalaraj, C. Viswanathan And N. Ponpandian, *Rsc Adv.*, 18 (2015) 13392.
40. C. Li, *J. Appl. Polym. Sci.*, 103 (2007) 3271.
41. G. Vasapollo , G. Mele , R. D. Sole , I. Pio, J. Li And S. E. Mazzetto, *Molecules*, 26 (2011) 5769.
42. E. Gholamrezapor, A . Eslami, *J MATER. SCI-MATER EL.*, 30 (2019) 4705.
43. M. M. Yu, J. Li, Sun, W. J. Sun, M. Jiang And F. X. Zhang, *J MATER. SCI.*, 49 (2014) 5519.
44. X. Zhao , Y. Wang, W. H. Feng, H. T. Lei And J. Li, *RSC Adv.*, 7 (2017) 52738
45. H. S. Yin, Y. L. Zhou, S. Y. Ai, X. G. Liu, L. S. Zhu And L. Lu, *Microchim Acta*., 169 (2010) 87.
46. J. Chen, G. Yang, M. Chen And W. Li, *Russ J Electrochem*., 45 (2009) 1287.
47. H. Wu, L. X. Guo, J. L. Zhang, S. L. Miao, C. L. He, B. Wang, Y. Q. Wu And Z. M. Chen, *Sensor Actuat B-Chem*., 230 (2016) 359.
48. Fernando. C. Moraes, Sonia. T. Tanimoto, G. R. S. Banda, S. A. S. Machado And L. H. Mascaro, *Electroanal*., 21(2010) 1091.